

Preparation, Crystal Structure, and Thermal Stability of the Cadmium Sulfide Nanoclusters $\text{Cd}_6\text{S}_4^{4+}$ and $\text{Cd}_2\text{Na}_2\text{S}^{4+}$ in the Sodalite Cavities of Zeolite A (LTA)

Seok Han Kim and Nam Ho Heo*

Laboratory of Structural Chemistry, Department of Applied Chemistry, Kyungpook National University, Daegu 702-701, Korea

Ghyung Hwa Kim

Pohang Accelerator Laboratory, POSTECH, Pohang 790-784, Korea

Suk Bong Hong

Division of Chemical Engineering, Hanbat National University, Daejeon 305-719, Korea

Karl Seff*

Department of Chemistry, University of Hawaii, 2545 The Mall, Honolulu, Hawaii 96822-2275

Received: June 3, 2006; In Final Form: October 12, 2006

The crystal structure and thermal stability of two cadmium sulfide nanoclusters prepared in zeolite A (LTA) have been studied by XPS, TGA, and single-crystal and powder XRD. The crystal structures of $[\text{Cd}_{2.4}\text{Na}_{3.2}(\text{Cd}_6\text{S}_4)_{0.4}(\text{Cd}_2\text{Na}_2\text{S})_{0.6}(\text{H}_2\text{O})_{\geq 5.8}][\text{Si}_{12}\text{Al}_{12}\text{O}_{48}]\text{-LTA}$ ($a = 12.2919(7)$ Å, crystal 1 (hydrated)) and $[\text{Cd}_4\text{Na}_2(\text{Cd}_2\text{O})(\text{Na}_2\text{O})][\text{Si}_{12}\text{Al}_{12}\text{O}_{48}]\text{-LTA}$ ($a = 12.2617(4)$ Å, crystal 2 (dehydrated)) were determined by single-crystal methods in the cubic space group $Pm\bar{3}m$ at 294(1) K. Crystal 1 was prepared by ion exchange of $\text{Na}_{12}\text{-LTA}$ in an aqueous stream 0.05 M in Cd^{2+} , followed by washing in a stream of water, followed by reaction in an aqueous stream 0.05 M in Na_2S . Crystal 2 was made by dehydrating crystal 1 at 623 K and 1×10^{-6} Torr for 3 days. In crystal 1, $\text{Cd}_6\text{S}_4^{4+}$ nanoclusters were found in and extending out of about 40% of the sodalite cavities. Central to each $\text{Cd}_6\text{S}_4^{4+}$ cluster is a Cd_4S_4 unit (interpenetrating Cd^{2+} and S^{2-} tetrahedra with near T_d symmetry, $\text{Cd-S} = 2.997(24)$ Å, $\text{Cd-S-Cd} = 113.8(12)^\circ$, and $\text{S-Cd-S} = 58.1(24)^\circ$). Each of the two remaining Cd^{2+} ions bonds radially through a 6-ring of the zeolite framework to a sulfide ion of this Cd_4S_4 unit ($\text{Cd-S} = 2.90(8)$ Å). In each of the remaining 60% of the sodalite cavities of crystal 1, a planar $\text{Cd}_2\text{Na}_2\text{S}^{4+}$ cluster was found ($\text{Cd-S/Na-S} = 2.35(5)/2.56(14)$ Å and $\text{Cd-S-Cd/Na-S-Na} = 122-(5)/92(7)^\circ$). $\text{Cd}_6\text{S}_4^{4+}$ and $\text{Cd}_2\text{Na}_2\text{S}^{4+}$ are stable within the zeolite up to about 700 K in air. Upon vacuum dehydration at 623 K, all sulfur was lost (crystal 2). Instead as anions, only two oxide ions remain per sodalite unit. One bridges between two Cd^{2+} ions (Cd_2O^{2+} , $\text{Cd-O} = 2.28(3)$ Å) and the other between two Na^+ ions (Na_2O , $\text{Na-O} = 2.21(10)$ Å).

1. Introduction

Zeolites are being used in various ways as advanced materials in the chemical and materials industries.^{1–9} In recent decades, zeolites, within their regular three-dimensionally arrayed pore and channel systems, have been found to be ideal hosts for the preparation and stabilization of unique-sized nanoclusters. These intrazeolitic clusters, uniform in size and regular in orientation, demonstrate quantum-size effects, affording them novel physical and chemical properties.^{7,10,11} Some of these clusters are much more stable within the zeolite, with respect to atmospheric moisture, for example, than nanoparticles (or thin films) synthesized neat.

Because of their potential applications, CdS clusters with quantum-size effects^{7,12} have been studied extensively. Their photophysical and photochemical properties in several porous media have been examined by spectroscopic methods.^{7,12–14}

Herron and Wang reported the optical properties of nanoclusters, less than 13 Å in size, of the semiconductors CdS and PbS encapsulated within zeolite Y (FAU) and mordenite (MOR).⁷ They observed a blue shift in the absorption threshold when the loading level and the mean size of the CdS clusters decreased.⁷ Stramel et al. also studied the spectral properties of very small clusters of CdS and PbS in zeolite X (FAU), sodalite (SOD), porous Vycor glass, and Laponite, a synthetic clay high in silica and magnesia.¹² They verified that the spectroscopic properties of these clusters are functions of their concentrations and sizes.¹² When the concentration and mean size of the CdS clusters in Laponite and porous Vycor decreased, the absorption onset in the reflectance absorption spectra exhibited a blue shift.

A number of synthetic methods have been used to prepare CdS nanoclusters in zeolites.^{9,14–16} These have been reviewed by Stramel et al.¹² They are commonly prepared within zeolites by impregnation methods or by cation-exchange followed by further treatment to introduce the anion.^{17,18} CdS clusters were prepared in zeolite Y by a conventional ion-exchange method

* Corresponding authors. E-mail: nhheo@mail.knu.ac.kr (N.H.H.); seff@hawaii.edu (K.S.).

TABLE 1: Experimental Conditions and Crystallographic Data

	(a) crystal 1 (hydrated)	(b) crystal 2 (dehydrated)
crystal (a cube) edge length (mm)	0.08	0.08
Cd ²⁺ ion exchange <i>T</i> (K), <i>t</i> (days), <i>V</i> (mL)	294, 3, 8	294, 3, 8
washing with deionized water <i>T</i> (K), <i>t</i> (days)	294, 1	294, 1
reaction of Cd-A with Na ₂ S <i>T</i> (K), <i>t</i> (days), <i>V</i> (mL)	294, 3, 5	294, 3, 5
dehydration <i>T</i> (K), <i>t</i> (days), <i>P</i> (Torr)		623, 3, 1 × 10 ⁻⁶
data collection <i>T</i> (K)	294(1)	294(1)
X-ray source	PLS(4A MXW BL) ^a	PLS(4A MXW BL) ^a
wavelength (Å)	0.82650	0.70000
space group, no.	<i>Pm</i> $\bar{3}$ <i>m</i> , 221	<i>Pm</i> $\bar{3}$ <i>m</i> , 221
unit cell constant, <i>a</i> (Å)	12.2919(7)	12.2617(4)
maximum 2 θ for data collection (deg)	61.93	61.93
no. of unique reflections measured, <i>m</i>	403	618
no. of reflections (<i>F</i> _o > 4 σ (<i>F</i> _o))	357	489
no. of variables, <i>s</i>	48	42
data/parameter ratio, <i>m/s</i>	8.4	14.7
weighting parameters : a/b	0.0626/7.6459	0.1022/1.6827
final error indices		
<i>R</i> ₁ ^b	0.0515	0.0608
<i>R</i> ₂ ^c	0.1336	0.1696
goodness of fit ^d	1.12	1.17

^a Beamline 4A MXW of the Pohang Light Source. ^b $R_1 = \sum |F_o - |F_c|| / \sum F_o$; R_1 is calculated using only the reflections for which $F_o > 4\sigma(F_o)$. ^c $R_2 = [\sum w(F_o^2 - F_c^2)^2 / \sum w(F_o^2)]^{1/2}$ is calculated using all unique reflections measured. ^d Goodness-of-fit = $(\sum w(F_o^2 - F_c^2)^2 / (m-s))^{1/2}$.

using aqueous CdCl₂ followed by treatment with H₂S gas.¹⁶ A more novel technique involved exposing a mechanical mixture of zeolite Y and CdCl₂·2.5H₂O to H₂S gas.¹⁶ Herron et al. prepared CdS clusters in zeolites A, X, and Y using aqueous Cd(NO₃)₂ followed by treatment with H₂S gas.⁹ Other sources of sulfur such as thiourea (H₂NCSNH₂)¹⁴ and aqueous Na₂S¹⁵ have also been used.

In all experimental work reported to date on “CdS clusters” in zeolites, those clusters have been inadequately characterized. In each case, the reference is simply to occluded CdS which could take many forms. It could be monomeric or polymeric, it could cluster with other atoms or not, and individual groupings could be neutral or carry a charge.

Because a knowledge of the structures and placements of the CdS clusters in zeolites is needed to understand their physical properties, some crystallographic and computational work has been undertaken.^{9,13} For CdS in zeolite Y, a combination of lattice-simulation and quantum-cluster calculations was used to predict the geometries and energies associated with possible CdS and CdO clusters and to explore the stabilities of Cd₄S₄ and Cd₄O₄ clusters with *T_d* symmetry in the sodalite cages.¹³ Cd₄X₄ clusters, where X is an undetermined mixture of S²⁻ and O²⁻ anions, were found inside the sodalite cages of zeolite Y using EXAFS and high-resolution X-ray powder diffraction methods.⁹

In this work, we have attempted to prepare CdS nanoclusters in a single crystal of zeolite A, to determine its composition by SEM-EDX analysis, to determine its structure and that of the nanoclusters within it by single-crystal X-ray diffraction methods, and to examine the thermal stability of those nanoclusters with regard to further applications by using a similarly prepared powder sample.

2. Experimental Section

2.1. Single-Crystal Experiments. Large colorless single crystals of zeolite 4A ([Na₁₂(H₂O)₂₇][Si₁₂Al₁₂O₄₈]-LTA, Na₁₂-A·27H₂O, Na₁₂-A, or Na-A) were synthesized by Kokotailo and Charnell.¹⁹ Its detailed structure was reported by Gramlich and Meier.²⁰ A single crystal of Na-A, a cube about 0.08 mm on an edge, was lodged in a fine Pyrex capillary. It was ion-exchanged by the dynamic (flow) method using a solution of Cd(NO₃)₂ (Aldrich 99.999%) and Cd(O₂CCH₃)₂ (Aldrich 99.99+%) (molar ratio 1:1 with a total Cd²⁺ concentration of 0.05 M) at

294 K for 3 d.²¹ The resulting colorless crystal was thoroughly washed with flowing deionized water at 294 K for 1 d to give Cd₆-A (or Cd-A),²¹ which was then placed in a flowing stream of aqueous 0.05 M Na₂S (Aldrich 99.99+%) solution at 294 K for 3 d.¹⁵ During this last step the crystal became very dark yellow, nearly black (crystal 1). (A second crystal prepared in this way was simply dark yellow.) It was then isolated in its capillary by sealing both ends with a small torch; no attempt was made, neither by evacuation nor heating, to remove solvent from the crystal.

X-ray diffraction data for crystal 1 were collected at 294(1) K on an ADSC Quantum210 detector at Beamline 4A MXW of The Pohang Light Source. The basic data file was generated by the program HKL2000 including the indexing program DENZO with the cubic space group *P*23. The cubic space group *Pm* $\bar{3}$ *m* (no systematic absences) was used in this work because reasons discussed previously^{22,23} were found to apply.

This very same crystal was then placed in another fine Pyrex capillary and was completely dehydrated at 623 K and 1 × 10⁻⁶ Torr for 3 d (crystal 2); a heating gradient of +25 K/h was used. After it was isolated in its capillary by sealing both ends with a small torch, it was seen to be pale yellow.

X-ray diffraction data for crystal 2 were collected as before. A summary of the experimental and crystallographic data for both compositions is presented in Table 1.

The crystal was then taken out of its capillary (exposed to the atmosphere) and attached to a piece of carbon attach tape for SEM-EDX and XPS analyses. The composition of the crystal was determined using a Horiba EMAX EDX (energy dispersive X-ray spectrometer) within a Hitachi S-4300SE FE-SEM (field emission scanning electron microscope) at 294 K and 1 × 10⁻⁷ Torr (see Figure 1). A comparison of the compositions as determined by crystallographic and SEM-EDX analyses are presented in Table 2.

Finally, to verify the chemical state of the cadmium species in the crystal, XPS experiments were performed on crystal 2 using a VG EXCALAB 250 instrument with Al K α (1486.7 eV) radiation for excitation (15 kV and 10 mA). Contamination was removed from the surface of the crystal by sputtering (removal rate = 0.6 Å/s) with an ion gun (3.0 kV) for 60 s. The resulting XPS spectrum for the Cd 3d electrons is shown in Figure 2.

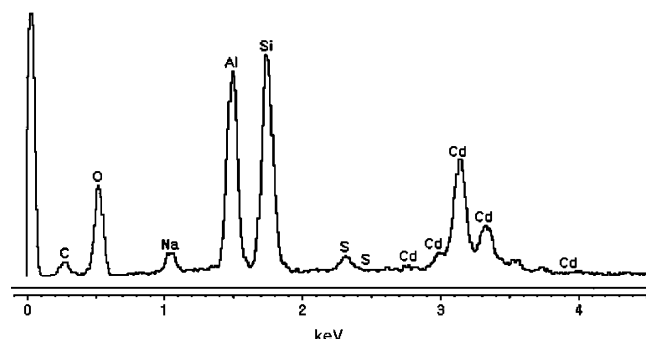


Figure 1. EDS spectra of $[\text{Cd}_4\text{Na}_2(\text{Cd}_2\text{O})(\text{Na}_2\text{O})][\text{Si}_{12}\text{Al}_{12}\text{O}_{48}]$ -LTA, crystal 2 (dehydrated).

2.2. Powder Experiments. Powder samples for XRD and TGA analyses were prepared using methods as similar as feasible to those used for the single crystal. Zeolite 4A powder ($[\text{Na}_{12}(\text{H}_2\text{O})_{27}][\text{Si}_{12}\text{Al}_{12}\text{O}_{48}]$ -LTA, Aldrich, 5 g) was placed in a flask. Hydrated Cd_6 -A was prepared by ion-exchange using 200 mL of $\text{Cd}(\text{NO}_3)_2$ (Aldrich >98%) and $\text{Cd}(\text{O}_2\text{CCH}_3)_2$ (Aldrich >98%) in the molar ratio 1:1 with a total Cd^{2+} concentration of 0.05 M at 294 K for 2 d. (By ICP analysis, the principal metal impurities in both cadmium salts in ppm are Ca 7.2, Pb 5.9, Na 1.8, Fe 1.2, Mg 1.1, B 0.2, and Ag 0.1.) The Cd^{2+} solutions were refreshed (replaced) every 6 h. The resulting powder was thoroughly washed with deionized water at 294 K for 1 d (Cd-A) and then placed in a solution of 0.05 M Na_2S (Aldrich 98%) at 294 K for 2 d with periodic replacement of the Na_2S solution. The Cd-A powder, initially white, became yellow (CdNaS-A) after treatment with Na_2S .

To determine the thermal stability of CdNaS-A, powder X-ray diffraction patterns were recorded after heating in air to various temperatures (see Figure 3). A Rigaku D/MAX 2000 with $\text{Cu K}\alpha$ radiation was used for this. CdNaS-A was heated from 293 to 1073 K with a heating gradient of +100 K/h; the sample was held at 673 and 1073 K for 1 h each. The diffraction pattern of Cd-A (hydrated) was also recorded (see Figure 3) so that the effect of the subsequent Na_2S treatment could be seen.

TGA experiments from 318 to 1073 K (+10 K/min) were done both in air and in nitrogen (see Figure 4) using a Perkin-Elmer Pyris Diamond TG/DTA instrument. The powder sample remained yellow after TGA analysis to 1073 K in nitrogen and TGA analysis to 673 K in air. During TGA analysis to 1073 K in air, however, it became white.

3. Structure Determination

3.1. $[\text{Cd}_{2.4}\text{Na}_{3.2}(\text{Cd}_6\text{S}_4)_{0.4}(\text{Cd}_2\text{Na}_2\text{S})_{0.6}(\text{H}_2\text{O})_{\geq 5.8}][\text{Si}_{12}\text{Al}_{12}\text{O}_{48}]$ -LTA (Crystal 1). Full-matrix least-squares refinement using SHELXL97²⁴ was done on F^2 using all reflections. It began with the atomic parameters of the framework atoms [(Si,Al), O(1), O(2), and O(3)] in Cd_6 -A.²⁵ Using isotropic thermal parameters, the initial refinement converged to the error indices (defined in footnotes to Table 1) $R_1 = 0.52$ and $R_2 = 0.83$. The progress of structure determination, as subsequent peaks were found on difference Fourier functions and identified as non-framework atoms, is given in Table 3a. The isotropic refinement of all 12 nonframework Fourier positions, with anisotropic refinement of the framework atoms, led to convergence with $R_1 = 0.045$ and $R_2 = 0.120$. The final cycles of refinement were carried out with occupancies fixed at the values given in Tables 3a and 4a; it converged to the final error indices $R_1 = 0.052$ and $R_2 = 0.134$. The final structural parameters are presented in Table 4a, and selected interatomic distances and angles are given in Table 5a.

3.2. $[\text{Cd}_4\text{Na}_2(\text{Cd}_2\text{O})(\text{Na}_2\text{O})][\text{Si}_{12}\text{Al}_{12}\text{O}_{48}]$ -LTA (Crystal 2). Least-squares refinement of the dehydrated crystal began as above. Using isotropic thermal parameters, the initial refinement converged to the error indices $R_1 = 0.48$ and $R_2 = 0.80$. The progress of structure determination as additional peaks were found on difference Fourier functions is given in Table 3b. Isotropic refinement of the nine non-framework and four framework positions converged to $R_1 = 0.066$ and $R_2 = 0.191$. For this, O(5) was refined at (0, y, z), the most general position that would allow it to be equidistant from two Na(1) ions, rather than (0, 0, z), the position found on the difference Fourier function. This is because the thermal parameter at O(5), when refined at (0, 0, z), was unrealistically high, $U_{\text{iso}} = 0.18(8) \text{ \AA}^2$ and because there is no physical reason for O(5) to be on a 4-fold axis. The error indices decreased further when the framework atoms were allowed to refine anisotropically: $R_1 = 0.056$ and $R_2 = 0.156$. The final cycles of refinement, carried out with occupancies fixed as given in Tables 3b and 4b, converged to $R_1 = 0.061$ and $R_2 = 0.170$. The final structural parameters are given in Table 4b, and selected interatomic distances and angles are given in Table 5b.

3.3. Weighting Scheme and Scattering Factors. Fixed weights were used initially for both crystals. The final weights were assigned using the formula $w = 1/[\sigma^2(F_o^2) + (aP)^2 + bP]$ where $P = [\text{Max}(F_o^2, 0) + 2F_c^2]/3$, with a and b as refined parameters (see Table 1). Atomic scattering factors for Cd^{2+} , Na^+ , S, O⁻, and (Si,Al)^{1.75+} were used.^{26,27} The function describing (Si,Al)^{1.75+} is the mean of the Si^{4+} , Si^0 , Al^{3+} , and Al^0 functions. All scattering factors were modified to account for anomalous dispersion.^{28,29} In the last cycles of least-squares refinement for both crystals, all shifts were less than 0.1% of their corresponding esds.

3.4. Distinguishing Na^+ and Cd^{2+} . Despite their low occupancy parameters, it has been possible to distinguish Na^+ and Cd^{2+} in this work. It is not by their distances to O^{2-} or S^{2-} ions, because the conventional ionic radii of Na^+ and Cd^{2+} are the same, 0.97 Å.³⁰ It is because Cd^{2+} (at. no. 50) scatters X-rays about $50/11 = 4.5$ times as much as Na^+ (at. no. 11), and because of the greater charge and greater covalency of Cd^{2+} , it is able to occupy the best sites (6-rings, and closer to their centers) within the zeolite. For example, replacing a Cd^{2+} ion in least-squares with Na^+ would lead to about 4.5 Na^+ , and charge balance could not be achieved. In addition, because the scattering factors of Na^+ and Cd^{2+} differ in character (not just scale), the thermal parameter would most likely become unrealistic. As another illustration, $\text{Cd}_6\text{S}_4^{4+}$ would become $\text{Na}_{26}\text{S}_4^{18+}$, which is chemically and crystallographically unacceptable.

4. Results and Discussion

4.1. All Cation to Framework Oxide Distances are Inaccurate. Each of the two structures presented in this work has five different 3-fold-axis cation positions. Because a 6-ring should adjust somewhat to the chemical nature and position of the cation it hosts, there should be five or more nonequivalent 6-rings in each structure, and five or more different O(3) positions should be present. These generally cannot be reliably resolved, so only a single O(3) position has been refined for each structure. Accordingly, all cation to O(3) distances are likely to be at least somewhat inaccurate, especially those involving cation positions of lower occupancy (because the crystallographically observed averaged 6-ring should be most like the one with the predominant cation position). The oxygen thermal parameters are all likely to be artificially elevated as

TABLE 2: Composition of Crystals 1 and 2 by Crystallographic and SEM-EDX Analysis

crystal	analysis method	Si		Al		Cd		Na		O				S		total	
		no. ^a	at % ^b	no.	at %	no.	at %	no.	at %	no.	no. of O _f ^c	no. of O _n ^d	at %	no.	at %	no.	at %
1 (hydr.)	XRD ^e	12.0	13.3	12.0	13.3	6.0	6.6	4.4	4.9	53.8	48.0 ^f	5.8	59.5	2.2	2.4	90.4	100
2 (dehydr.)	XRD ^e	12.0	14.3	12.0	14.3	6.0	7.1	4.0	4.8	50.0	48.0 ^f	2.0	59.5	0	0	84.0	100
2 (dehydr.)	EDX ^g		15.3		12.9		5.4		2.7				62.8		0.9 ^h		100

^a Number of atoms per unit cell. ^b Atomic percent of the element. ^c Framework oxygen. ^d Nonframework oxygen. ^e Composition determined by least-squares refinement of single-crystal diffraction data. ^f Fixed. ^g Composition determined by SEM-EDX. ^h See section 4.4.

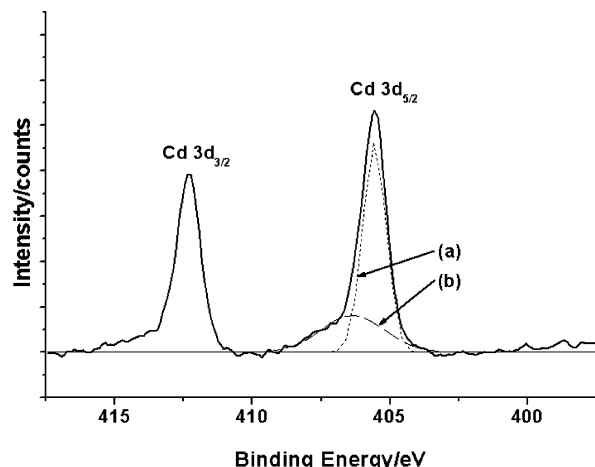


Figure 2. XPS spectra of $[\text{Cd}_4\text{Na}_2(\text{Cd}_2\text{O})(\text{Na}_2\text{O})][\text{Si}_{12}\text{Al}_{12}\text{O}_{48}]\text{-LTA}$, crystal 2 (dehydrated): (a) sub-peak at 405.6 eV; (b) sub-peak at 406.4 eV.

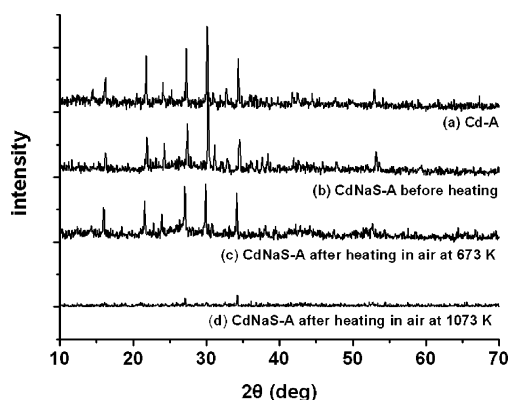


Figure 3. X-ray diffraction patterns of the powder samples.

they refine to better describe the electron density about those positions. These inaccuracies have not been incorporated into the crystallographic esds. (For the hydrated crystal, some cation-to-O(3) distances may be unusually long because that cation may coordinate to a water molecule.)

4.2. Crystal Structure of $[\text{Cd}_{2.4}\text{Na}_{3.2}(\text{Cd}_6\text{S}_4)_{0.4}(\text{Cd}_2\text{Na}_2\text{S})_{0.6}(\text{H}_2\text{O})_{\geq 5.8}][\text{Si}_{12}\text{Al}_{12}\text{O}_{48}]\text{-LTA}$ (Crystal 1). Per unit cell, a total of 6.0 Cd^{2+} and 4.4 Na^+ cations are found distributed over eight crystallographically distinct positions. Five of these eight are 3-fold-axis positions near 6-rings. Here 1.6, 1.8, 1.8, and 0.8 Cd^{2+} ions occupy the Cd(1), Cd(2), Cd(3), and Cd(4) positions, respectively (see Figures 5 and 6), and 0.8 Na^+ are found at Na(1) (see Figure 5). The remaining cations, all Na^+ , occupy 4-ring and 8-ring positions. In 8-rings at Na(2), 0.8 Na^+ ions are found, and opposite 4-rings in the large cavities at Na(3) are 1.6 Na^+ ions (see Figure 5). Finally, 1.2 Na^+ ions at Na(4) lie opposite 4-rings in the sodalite cavities (see Figure 7).

The 3-fold-axis Cd^{2+} positions, Cd(n), $n = 1-4$, are each 2.347(5), 2.219(5), 2.201(5), and 2.322(7) Å, respectively, from three O(3) oxygens of a 6-ring. These distances are close to the

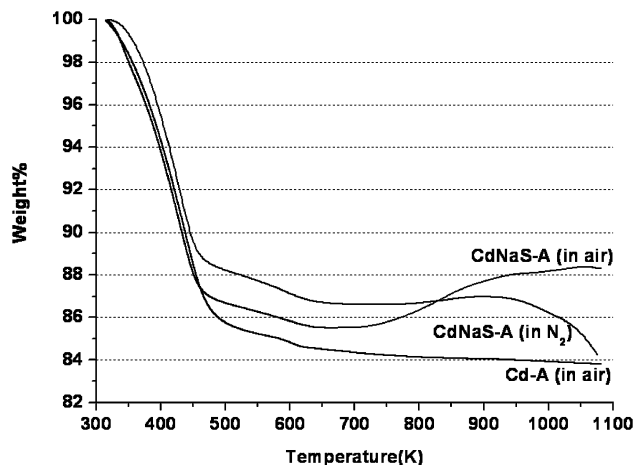


Figure 4. TGA graphs of the powder samples.

sum of the ionic radii of Cd^{2+} and O^{2-} , $0.97 + 1.32 \text{ Å} = 2.29 \text{ Å}$.³⁰ and are similar to those found in previous work (2.16–2.39 Å).^{21,25} The approach distances of the 3-fold-axis Na^+ ion, Na(1), to its three O(3) oxygens, 2.65(8) Å (see Figure 5), is somewhat longer than the sum of the ionic radii of Na^+ and O^{2-} , also $0.97 + 1.32 \text{ Å} = 2.29 \text{ Å}$,³⁰ perhaps because Na(1) coordinates to a water molecule at O(5) and because (it is proposed later in this section) Na(1) is repelled by $\text{Cd}_6\text{S}_4^{4+}$. In dehydrated $\text{Na}_{12}\text{-A}$, the Na–O distances range from 2.32 to 2.47 Å.³¹ The displacements of these ions from the (111) planes at O(3) are given in Table 6.

Each Na^+ ion at Na(2) is 2.20(31) Å from one O(1) oxygen and 2.77(12) Å from two O(2) oxygens of the same 8-ring (see Figure 5). The shorter distance is similar to that seen in dehydrated $\text{Na}_{12}\text{-A}$,³¹ 2.40(6) Å, and is in agreement with the sum of ionic radii of Na^+ and O^{2-} , 2.29 Å.³⁰ Each of the Na^+ ions at Na(3) is 2.86(11) Å from two O(1) oxygens and 2.96–(10) Å from two O(3) oxygens; these distances are close to that seen in hydrated $\text{Na}_{12}\text{-A}$,²⁰ 3.16(1) Å. The Na^+ ions at Na(4) are also quite far, 2.94(13) Å, from four framework oxygens at O(3) perhaps because each of these Na^+ ions bonds strongly (primarily) to a sulfide anion (see below).

Because the total charge of the exchangeable cations per unit cell, 16.4+ (12+ for the 6.0 Cd^{2+} ions + 4.4+ for the 4.4 Na^+ ions), exceeds that needed to balance the anionic charge of the zeolite framework, 12–, guest anions with a total charge of 4.4– per unit cell must be present. Providing this balance are 2.2 S^{2-} anions per unit cell at two crystallographically distinct positions in the sodalite cavities, 1.6 at S(1) and 0.6 at S(2). (See section 4.4 for a discussion of the analytical (EDX) support for this value.)

The Cd(1)–S(1) distance, 2.997(24) Å, is only a little longer than the sum of ionic radii of Cd^{2+} and S^{2-} , $0.97 + 1.84 \text{ Å} = 2.81 \text{ Å}$,³⁰ and is reasonable. Because the occupancies at Cd(1) and S(2) appear to be equal, and because both ions are relatively far from framework atoms, they appear to bond to each other.

Each sulfide ion at S(2) in the sodalite unit is 2.35(5) Å from two Cd^{2+} ions at Cd(2), substantially less than the sum of the

TABLE 3: Steps of Structure Determination as Nonframework Atomic Positions Were Found

(a) crystal 1 (hydrated)														
step/ atom	number of atoms or ions per unit cell												error indices ^d	
	Cd(1)	Cd(2)	Cd(3)	Cd(4)	Na(1)	Na(2)	Na(3)	Na(4)	S(1)	S(2)	O(4)	O(5)	R ₁	R ₂
1 ^a													0.52	0.83
2		5.9											0.31	0.70
3		3.7	2.6										0.17	0.42
4		2.1	2.2	1.8									0.088	0.230
5 ^b	1.5	2.3	1.5	0.9									0.072	0.196
6 ^b	1.5	2.2	1.4	0.7					4.0				0.059	0.152
7 ^b	1.5	2.2	1.4	0.7	1.0				4.0				0.055	0.145
8 ^b	1.4	2.2	1.4	0.7	1.0	0.7			4.3				0.055	0.144
9 ^b	1.5	2.2	1.4	0.7	1.0	0.7			4.2	0.2			0.053	0.142
10 ^b	1.4	2.2	1.4	0.7	1.5	0.9	1.1		4.3	0.2			0.052	0.137
11 ^b	1.5	2.2	1.4	0.8	2.1	1.2	1.3		3.7	0.2		5.1	0.049	0.126
12 ^b	1.1	1.6	1.6	1.2	1.4	1.2	1.2		3.5	0.2	2.3	5.1	0.048	0.123
13 ^b	1.3	1.7	1.5	1.1	1.2	1.2	1.5	3.2	1.4	0.4	2.2	5.1	0.0453	0.1195
14 ^{b,c}	1.6	1.8	1.8	0.8	0.8	0.8	1.6	1.2	1.6	0.6	1.8	4.0	0.0515	0.1336
(b) crystal 2 (dehydrated)														
step/atom	number of atoms or ions per unit cell										error indices ^d			
	Cd(1)	Cd(2)	Cd(3)	Cd(4)	Cd(5)	Na(1)	Na(2)	O(4)	O(5)	R ₁	R ₂			
1 ^a										0.48	0.80			
2		3.4								0.26	0.64			
3		3.0	2.1							0.15	0.42			
4	2.5	0.9	1.4							0.11	0.31			
5	1.9	1.1	1.0				3.7			0.093	0.260			
6	2.1	0.7	1.0			2.5	2.2			0.093	0.256			
7	2.1	0.7	1.1	1.2		0.8	2.2			0.078	0.223			
8	2.1	0.7	1.1	1.3	1.0	1.5	2.0			0.073	0.205			
9	2.0	0.7	1.1	1.1	0.8	1.9	2.3	1.7		0.067	0.196			
10	2.0	0.7	1.1	1.1	0.7	1.9	2.2	1.6	1.3	0.066	0.191			
11 ^b	2.0	0.7	1.1	1.1	0.7	1.9	2.1	1.5	1.5	0.0562	0.1564			
12 ^{b,c}	2.0	1.0	1.0	1.0	1.0	2.0	2.0	1.0	1.0	0.0608	0.1696			

^a Only the atoms of the zeolite framework were present in the initial structure model. They were refined isotropically. ^b Framework atoms were allowed to refine anisotropically. ^c Fixed occupancies are used for all atoms. ^d Defined in footnotes to Table 1.

corresponding ionic radii, 2.81 Å.³⁰ It is also 2.56(14) Å from two Na⁺ ions at Na(4) (see Figure 7). The latter distances do not differ significantly from the sum of the ionic radii of Na⁺ and S²⁻, also 0.97 + 1.84 Å = 2.81 Å.³⁰ Except for these two Na⁺ ions, S(2) has only the two Cd²⁺ ions at Cd(2) to bond to (see Figure 7); perhaps this is responsible for the short S(2)–Cd(2) bonds.

There are 1.6 CdS and 0.6 Cd₂Na₂S formula units per unit cell and therefore per sodalite cavity. This CdS occupancy requires that CdS clusters at least as large as Cd₂S₂ must be present in some sodalite cavities. Further clustering of the CdS formula units is readily possible up to Cd₄S₄, which also shows the most satisfactory coordination for both Cd and S. The Cd₂-Na₂S units cannot cluster further, however (see Figure 7), so 0.6 sodalite cavities must contain Cd₂Na₂S. (Further clustering to give Cd₄Na₂S₂⁶⁺ with bridging Na⁺ ions would have a stoichiometry that would not fit the crystallographic results as well, and two Cd₂Na₂S⁴⁺ units per sodalite cavity would require four unacceptably close Na⁺...Na⁺ contacts, Na(4)–Na(4) = 2.60 Å.) Therefore, the maximally clustered Cd₄S₄ group must occur in the remaining 0.4 (1.6/0.4 = 4) sodalite cavities, and all sodalite cavities must have content, either Cd₄S₄ or Cd₂-Na₂S. (For Cd₄S₄ to cluster further would require an impossibly close Cd(1)–S(1) approach (1.29(8) Å) for ions on the same 3-fold axis; Cd₄S₄ effectively fills a sodalite cavity.) (Further clustering of Cd₂Na₂S units would now require that some sodalite cavities contain no cluster at all.) Anticipating a similar diversity for the large cavities, we identify two kinds of unit cells, UC1 (40%, Cd₄S₄) and UC2 (60%, Cd₂Na₂S) (see Table 7).

The Cd₄S₄ cluster has an interpenetrating tetrahedral (puckered cubic, symmetry *T_d*) structure (see Figures 8 and 9). In contrast to what a smaller cluster would afford, it completes an octahedral coordination environment for each Cd²⁺ ion and justifies the symmetry of the Cd(1) and S(1) positions. In this arrangement, each Cd²⁺ ion would bond to three S²⁻ ions and each S²⁻ ion would bond to three Cd²⁺ ions (Cd(1)–S(1) = 2.997(24) Å, Cd(1)–S(1)–Cd(1) = 113.8(12)°, S(1)–Cd(1)–S(1) = 58.1(24)°, see Table 5a). It is held firmly in place by the interactions of its four tetrahedrally arranged Cd²⁺ ions with 12 6-ring oxygens (Cd(1)–O(3) = 2.347(5) Å). The octahedral coordination about each Cd(1) ion is trigonally distorted (see Figure 8).

Surrounding each Cd₄S₄ cluster are two Cd²⁺ ions at Cd(4) and two Na⁺ ions at Na(1) in the large cavity (see Figure 8). To avoid unacceptably short approaches to the cations at Cd(1), they must lie opposite the four sodalite-cavity S²⁻ anions at S(1). The ions at Cd(4) bond radially to S(1), S(1)–Cd(4) = 2.90(8) Å, as compared to 2.81 Å,³⁰ the sum of the corresponding ionic radii, extending the Cd₄S₄ clusters to Cd₆S₄⁴⁺ (see Figures 8 and 9). The ions at Na(1), in contrast, appear not to bond significantly to S(1) of the now highly cationic (and covalent) Cd₆S₄⁴⁺ cluster. The Na(1)–S(1) distance, 3.62(15) Å, is significantly longer than 2.81 Å,³⁰ the sum of the corresponding radii. The Na(1) position extends significantly farther than Cd(4) into the large cavity, and is even farther, 2.65(8) Å, than the sum of the corresponding radii, 2.29 Å,³⁰ from O(3). Because Cd₆S₄⁴⁺ cannot have *T_d* symmetry (see Figure 9), the Cd₄S₄ group at its core also should not. S(1) in particular

TABLE 4: Positional, Thermal, and Occupancy Parameters^a

											occupancy ^b	
atoms	Wyckoff position	x	y	z	U ₁₁ or U _{iso}	U ₂₂	U ₃₃	U ₂₃	U ₁₃	U ₁₂	varied	fixed
(a) crystal 1 (hydrated)												
(Si,Al)	24(k)	0	1827(1)	3689(1)	130(10)	130(10)	94(10)	14(6)	0	0		24 ^c
O(1)	12(h)	0	2051(6)	5000 ^d	561(42)	482(40)	378(37)	0	0	0		12
O(2)	12(i)	0	2933(4)	2933(4)	444(36)	337(21)	337(21)	112(27)	0	0		12
O(3)	24(m)	1112(3)	1112(3)	3295(4)	371(16)	371(16)	439(27)	45(15)	45(15)	77(19)		24
Cd(1)	8(g)	1445(4)	1445(4)	1445(4)	428(18)						1.3(2)	1.6
Cd(2)	8(g)	1675(3)	1675(3)	1675(3)	175(9)						1.7(3)	1.8
Cd(3)	8(g)	1936(5)	1936(5)	1936(5)	368(14)						1.5(2)	1.8
Cd(4)	8(g)	2200(7)	2200(7)	2200(7)	211(19)						1.1(2)	0.8
Na(1)	8(g)	2539(65)	2539(65)	2539(65)	1003(267)						1.2(6)	0.8
Na(2)	12(h)	0	3840(251)	5000 ^d	3667(1901)						1.2(5)	0.8
Na(3)	12(j)	2315(81)	2315(81)	5000 ^d	2485(485)						1.5(5)	1.6
Na(4)	6(e)	0	0	1495(143)	2898(648)						3.2(8) ^e	1.2
S(1)	8(g)	837(38)	837(38)	837(38)	2086(262)						1.4(5)	1.6
S(2)	12(i)	0	1024(61)	1024(61)	961(249)						0.4(3)	0.6
O(4)	8(g)	3102(34)	3102(34)	3102(34)	832(178)						2.2(4)	1.8
O(5)	48(n)	2074(67)	3836(70)	4477(64)	1598(389)						5.1(10)	4.0
(b) crystal 2 (dehydrated)												
(Si,Al)	24(k)	0	1824(1)	3688(1)	136(6)	117(6)	91(6)	9(4)	0	0		24 ^c
O(1)	12(h)	0	2077(5)	5000 ^d	583(33)	525(32)	343(24)	0	0	0		12
O(2)	12(i)	0	2948(3)	2948(3)	578(31)	366(16)	366(16)	102(20)	0	0		12
O(3)	24(m)	1120(2)	1120(2)	3296(3)	413(12)	413(12)	443(19)	31(11)	31(11)	59(15)		24
Cd(1)	8(g)	1558(2)	1558(2)	1558(2)	237(6)						2.0(1)	2.0
Cd(2)	8(g)	1857(6)	1857(6)	1857(6)	527(17)						0.7(1)	1.0
Cd(3)	8(g)	2165(4)	2165(4)	2165(4)	335(12)						1.1(1)	1.0
Cd(4)	12(i)	0	4441(17)	4441(17)	2501(162)						1.1(1)	1.0
Cd(5)	24(l)	1453(32)	3577(34)	5000 ^d	2005(155)						0.7(1)	1.0
Na(1)	8(g)	1383(7)	1383(7)	1383(7)	188(36)						1.9(7)	2.0
Na(2)	8(g)	2378(7)	2378(7)	2378(7)	262(32)						2.1(4)	2.0
O(4)	12(i)	0	836(31)	836(31)	379(113)						1.5(2)	1.0
O(5)	24(k)	0	286(124)	1724(66)	811(440)						1.5(4)	1.0

^a Positional and thermal parameters $\times 10^4$ are given. Numbers in parentheses are the estimated standard deviations in the units of the least significant digit given for the corresponding parameter. The anisotropic temperature factor is $\exp[-2\pi^2 a^{-2}(U_{11}h^2 + U_{22}k^2 + U_{33}l^2 + 2U_{12}hk + 2U_{13}hl + 2U_{23}kl)]$. ^b Occupancy factors are given as the number of atoms or ions per unit cell. ^c Occupancy for (Si) = 12, occupancy for (Al) = 12. ^d Exactly 0.5 by symmetry. ^e The environment about Na(4) does not require it to be on a 4-fold axis (at Wyckoff 6(e)). Attempts to refine Na(4) at a more general position were not successful. To compensate for its likely displacement from 6(e), Na(4) appears to have refined to a thermal parameter that is too large. Then, due to the customary positive correlation in least-squares between the thermal and occupancy parameters, the occupancy parameter is likely to have also refined to a value that is too large.

must be an average of two positions; these could not be resolved in this work.

At two positions, 5.8 oxygen atoms per unit cell, presumably oxygens of water molecules, are found. On 3-fold axes in the large cavity coordinating at 2.48(7) Å to Cd^{2+} ions at Cd(3) are 1.8 oxygen atoms at O(4) (see Figure 6); the sum of the corresponding radii is 2.29 Å.³⁰ To avoid a 1.05-Å Cd(1)–Cd(3) distance, these Cd(3) ions must occupy unit cell 2 (UC2). Therefore, three (1.8/0.6 = 3) O(4) molecules coordinate to the three Cd(3) ions in each large cavity of UC2.

Opposite 4-rings in the large cavity are 4.0 oxygen atoms at O(5) (see Figure 5). Because each of these can be 2.63(9) Å from Na(2) and 2.00(11) Å from Na(3) (the sum of the corresponding radii is 2.29 Å³⁰), the molecules at O(5) can coordinate to either or both of them. They may also hydrogen bond among themselves (O(5)–O(5) = 2.86(17) and 3.06(16) Å). Na(2) and Na(3) are placed in UC1 because its cationic charge is only 6+ at this point; UC2 already has a total charge of 12+ (three Cd(2), three Cd(3), two Na(4), and one S(2) ion, see Table 7). Because O(5) must coordinate to Na(2) and/or Na(3) ions, ten (4.0/0.4 = 10) O(5) oxygen atoms are likely to be in the large cavity of UC1. In pairs they coordinate to the four Na⁺ ions at Na(3) (Na(3)–O(5) = 2.00(11) Å) on 2-fold axes opposite 4-rings (see Figure 5). Because each O(5) molecule can make two hydrogen bonds to other O(5) molecules and every Na(3) ion bonds to two O(5) atoms, a 12-membered $\text{Na}_4(\text{H}_2\text{O})_8^{4+}$ ring appears to be present in the large cavity of

UC1 (see Figure 5). Two of these O(5) molecules per UC1 can also coordinate to a Na(2) ion which would lie in the one 8-ring per UC1 that is not occupied by a $\text{Na}_4(\text{H}_2\text{O})_8^{4+}$ ring. The other Na⁺ ion at Na(2) might associate itself with a water molecule of the $\text{Na}_4(\text{H}_2\text{O})_8^{4+}$ ring.

In the sodalite units of UC2, three Cd^{2+} ions at Cd(2), two Na⁺ ions at Na(4), and one sulfide ion at S(2) are found (see Table 7). Without one Cd(2) ion, which is on 3-fold axes in the sodalite unit, these form a $\text{Cd}_2\text{Na}_2\text{S}^{4+}$ cluster in each sodalite unit of UC2 (see Figure 7). The sulfide ion at S(2) is 2.35(5) Å from two Cd^{2+} ions at Cd(2) and 2.56(14) Å from two Na⁺ ions at Na(4) ((Cd(2)–S(2)–Cd(2) = 122(5)°, Cd(2)–S(2)–Na(4) = 73(3)°, Na(4)–S(2)–Na(4) = 92(7)°). The sum of the angles about S(2), 122° + 2 × 73° + 92° = 360°, indicates that this cluster is planar; this is easily seen in Figure 7.

Cationic clusters like $\text{Cd}_6\text{S}_4^{4+}$ and $\text{Cd}_2\text{Na}_2\text{S}^{4+}$ are commonly found in the anionic sodalite cavities of zeolites; a brief review is available.²¹ For example, Na_4^{3+} was found in zeolite Y (FAU),³² S_4^{4+} was found in zeolite X (FAU),²¹ and In_5^{7+} was found in zeolites A (LTA)³³ and X (FAU).³⁴ The clusters Zn_5^{6+} and *cyclo*- Zn_6^{8+} have been proposed in the product of the reaction of zeolite H–Y (FAU) with Zn(g).³⁵ Cationic $\text{Pb}_8\text{O}_4^{n+}$ clusters were found in zeolite X (FAU),³⁶ and $\text{Cd}_8\text{O}_4^{8+}$ and Pb_2S^{2+} ³⁸ clusters were reported in zeolite Y (FAU). Crystal 2 (this report) contains Cd_2O^{2+} . The smaller of the above cationic clusters lie entirely within sodalite cavities, like $\text{Cd}_2\text{Na}_2\text{S}^{4+}$. The

TABLE 5: Selected Interatomic Distances (Å) and Angles (deg)^a

(a) crystal 1 (hydrated)			
(Si,Al)–O(1)	1.635(2)	O(1)–(Si,Al)–O(2)	114.6(3)
(Si,Al)–O(2)	1.647(2)	O(1)–(Si,Al)–O(3)	111.6(2)
(Si,Al)–O(3)	1.695(2)	O(2)–(Si,Al)–O(3)	105.5(2)
		O(3)–(Si,Al)–O(3)	107.5(3)
Cd(1)–O(3)	2.347(5)		
Cd(2)–O(3)	2.219(5)	(Si,Al)–O(1)–(Si,Al)	160.6(5)
Cd(3)–O(3)	2.201(5)	(Si,Al)–O(2)–(Si,Al)	158.7(5)
Cd(4)–O(3)	2.322(7)	(Si,Al)–O(3)–(Si,Al)	139.0(3)
Na(1)–O(3)	2.65(8)		
Na(2)–O(1)	2.20(31)	O(3)–Cd(1)–O(3)	107.9(2)
Na(2)–O(2)	2.77(12)	O(3)–Cd(2)–O(3)	117.5(1)
Na(3)–O(1)	2.86(11)	O(3)–Cd(3)–O(3)	119.2(1)
Na(3)–O(3)	2.96(10)	O(3)–Cd(4)–O(3)	109.7(3)
Na(4)–O(3)	2.94(13)	O(3)–Na(1)–O(3)	91(3)
		O(1)–Na(2)–O(2)	66(6)
Cd(1)–S(1)	2.997(24)		
Cd(2)–S(2)	2.35(5)	S(1)–Cd(1)–S(1)	58.1(24)
Cd(3)–O(4)	2.48(7)	S(1)–Cd(1)–O(3)	92.0(9)/145.1(14)
Cd(4)–S(1)	2.90(8)	S(2)–Cd(2)–O(3)	85.8(12)/125.1(23)
Na(1)–O(5)	2.92(12)	O(3)–Cd(3)–O(4)	95.3(3)
Na(2)–O(5)	2.63(9)	O(1)–Na(2)–O(5)	90(7)
Na(3)–O(5)	2.00(11)	O(1)–Na(3)–O(5)	88(3)/156(5)
Na(4)–S(2)	2.56(14)	O(3)–Na(3)–O(5)	100(3)/128(3)
O(5)–O(5)	2.86(17)	Cd(1)–S(1)–Cd(1)	113.8(12)
		Cd(2)–S(2)–Cd(2)	122(5)
S(1)···S(1)	2.91(6)	Cd(2)–S(2)–Na(4)	73(3)
S(1)···O(3)	3.06(6)	Na(4)–S(2)–Na(4)	92(7)
S(2)···O(3)	3.11(7)	Na(3)–O(5)–O(5)	159(3)
O(5)···O(1)	3.42(9)		
O(5)···O(2)	3.37(8)		
O(4)···O(3)	3.47(6)		
(b) crystal 2 (dehydrated)			
(Si,Al)–O(1)	1.639(2)	O(1)–(Si,Al)–O(2)	112.4(3)
(Si,Al)–O(2)	1.650(2)	O(1)–(Si,Al)–O(3)	112.1(2)
(Si,Al)–O(3)	1.692(2)	O(2)–(Si,Al)–O(3)	105.7(2)
		O(3)–(Si,Al)–O(3)	108.6(3)
Cd(1)–O(3)	2.262(4)		
Cd(1)–O(2)	3.076(4)	(Si,Al)–O(1)–(Si,Al)	158.2(4)
Cd(2)–O(3)	2.178(4)	(Si,Al)–O(2)–(Si,Al)	156.6(4)
Cd(2)–O(2)	2.961(4)	(Si,Al)–O(3)–(Si,Al)	138.4(2)
Cd(3)–O(3)	2.281(5)		
Cd(3)–O(2)	2.982(3)	O(3)–Cd(1)–O(3)	113.0(1)
Cd(4)–O(2)	2.586(30)	O(3)–Cd(2)–O(3)	120.0(1)
Cd(4)–O(1)	2.979(16)	O(3)–Cd(3)–O(3)	111.5(2)
Cd(5)–O(1)	2.560(42)	O(3)–Na(1)–O(3)	104.3(4)
Cd(5)–O(2)	3.177(24)	O(3)–Na(2)–O(3)	100.5(4)
Na(1)–O(3)	2.389(7)	O(3)–Na(1)–O(5)	68.2(21)/121(3)/134(3)
Na(1)–O(2)	3.201(7)	O(3)–Cd(1)–O(4)	94.3(6)/127.2(11)
Na(2)–O(3)	2.454(8)		
Na(2)–O(2)	3.079(5)	Cd(1)–O(4)–Cd(1)	113.5(22)
		Na(1)–O(5)–Na(1)	101(6)
Cd(1)–O(4)	2.28(3)		
Na(1)–O(5)	2.21(10)		
O(5)···O(3)	2.58(8)		
O(4)···O(3)	3.33(4)		
O(5)···O(4)	3.43(9)		

^a The numbers in parentheses are the estimated standard deviations in the units of the least significant digit given for the corresponding parameter.

larger clusters, like $\text{Cd}_6\text{S}_4^{4+}$, are centered within, yet extend out of, sodalite cavities.

It may be expected that further successive treatments of crystal 1 with aqueous Cd^{2+} followed by aqueous Na_2S , ending with aqueous Cd^{2+} , would have decreased its Na^+ content and increased its concentration of CdS clusters, perhaps still $\text{Cd}_6\text{S}_4^{4+}$.

Considering the crystallographic uncertainties that result from the low occupancies involved, their resolution into $\text{Cd}_6\text{S}_4^{4+}$ and $\text{Cd}_2\text{Na}_2\text{S}^{4+}$ cannot be considered proven. Three or more nonequivalent clusters might exist. However, the reasonableness

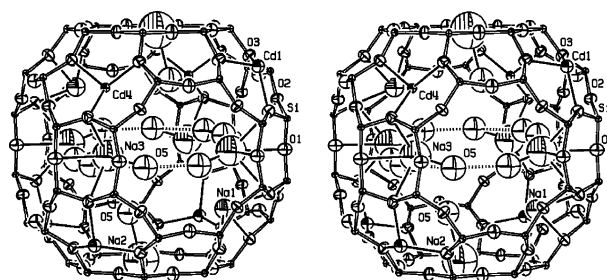


Figure 5. Stereoview of the large cavity of unit cell 1 (UC1) in $|\text{Cd}_{2.4}\text{-Na}_{3.2}(\text{Cd}_6\text{S}_4)_{0.4}(\text{Cd}_2\text{Na}_2\text{S})_{0.6}(\text{H}_2\text{O})_{\geq 5.8}|[\text{Si}_{12}\text{Al}_{12}\text{O}_{48}]\text{-LTA}$, crystal 1 (hydrated). The zeolite framework is drawn using relatively thick bonds. Ellipsoids of 20% probability are shown.

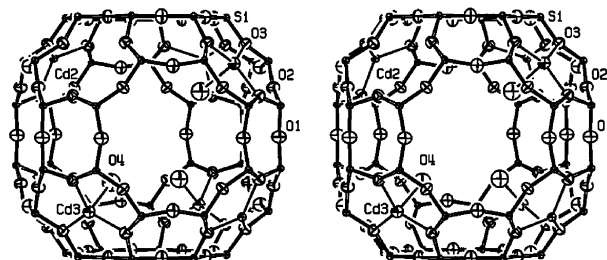


Figure 6. Stereoview of the large cavity of unit cell 2 (UC2) in $|\text{Cd}_{2.4}\text{-Na}_{3.2}(\text{Cd}_6\text{S}_4)_{0.4}(\text{Cd}_2\text{Na}_2\text{S})_{0.6}(\text{H}_2\text{O})_{\geq 5.8}|[\text{Si}_{12}\text{Al}_{12}\text{O}_{48}]\text{-LTA}$, crystal 1 (hydrated). See the caption to Figure 5 for other details.

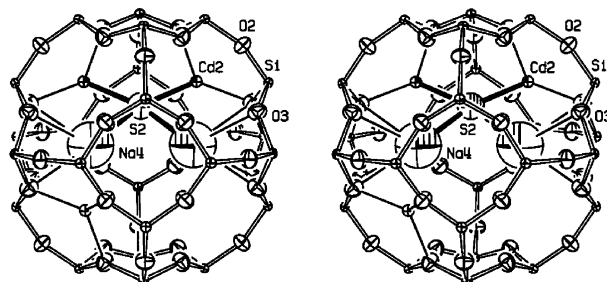


Figure 7. Stereoview of the sodalite unit of unit cell 2 (UC2) in $|\text{Cd}_{2.4}\text{-Na}_{3.2}(\text{Cd}_6\text{S}_4)_{0.4}(\text{Cd}_2\text{Na}_2\text{S})_{0.6}(\text{H}_2\text{O})_{\geq 5.8}|[\text{Si}_{12}\text{Al}_{12}\text{O}_{48}]\text{-LTA}$, crystal 1 (hydrated), containing a planar $\text{Cd}_2\text{Na}_2\text{S}^{4+}$ cluster. See the caption to Figure 5 for other details.

TABLE 6: Deviations of Atoms (Å) from the (111) Plane at O(3)^a

	crystal 1	crystal 2	crystal 1	crystal 2
Cd(1)	−0.84	−0.60	Na(1)	1.49
Cd(2)	−0.35	0.04	Na(2)	−0.97
Cd(3)	0.21	0.69	S(1)	1.15
Cd(4)	0.77		O(4)	−2.13
				2.69

^a A negative deviation indicates that the atom lies on the same side of the plane as the origin, i.e., inside the sodalite unit.

of the geometries of the two clusters presented, the result that every sodalite cavity contains one cluster, and the thermodynamic expectation that only those clusters of lowest energy should form, argue for the two-cluster model herein presented.

The cationic clusters $\text{Cd}_6\text{S}_4^{4+}$ and $\text{Cd}_2\text{Na}_2\text{S}^{4+}$ appear to be new to chemistry. Earlier work discussed in section 1 had reported Cd_4X_4 clusters or subunits,⁹ where X is an undetermined mixture of S^{2-} and O^{2-} , and that may have been a fraction of a larger cluster, such as $\text{Cd}_6\text{X}_4^{4+}$. Computational work established that the lowest energy structure for Cd_4S_4 in the sodalite cavity of zeolite Y had symmetry T_d ;¹³ cationic clusters such as $\text{Cd}_6\text{S}_4^{4+}$ were not considered.

4.3. Crystal Structure of $|\text{Cd}_4\text{Na}_2(\text{Cd}_2\text{O})(\text{Na}_2\text{O})|[\text{Si}_{12}\text{Al}_{12}\text{O}_{48}]\text{-LTA}$ (Crystal 2). The flex of (angles in) the framework

TABLE 7: Distribution of Nonframework Atoms (Cd, Na, O, and S) in the Component Unit Cells of Crystal 1

atoms	position	charge	unit cell 1 (40%)		unit cell 2 (60%)		total (averaged)		
			no.	charge	no.	charge	no.	charge	varied no.
(a) as individual ions or atoms									
Cd(1)	opposite 6-ring ^{b,c}	+2	4	+8	0	0	1.6	+3.2	1.3(2)
Cd(2)	opposite 6-ring ^{b,c}	+2	0	0	3	+6	1.8	+3.6	1.7(3)
Cd(3)	opposite 6-ring ^{a,b}	+2	0	0	3	+6	1.8	+3.6	1.5(2)
Cd(4)	opposite 6-ring ^{a,b}	+2	2	+4	0	0	0.8	+1.6	1.1(2)
Na(1)	opposite 6-ring ^{a,b}	+1	2	+2	0	0	0.8	+0.8	1.2(6)
Na(2)	8-ring ^a	+1	2	+2	0	0	0.8	+0.8	1.2(5)
Na(3)	opposite 4-ring ^a	+1	4	+4	0	0	1.6	+1.6	1.5(5)
Na(4)	opposite 4-ring ^c	+1	0	0	2	+2	1.2	+1.2	3.2(8)
S(1)	opposite 6-ring ^{b,c}	-2	4	-8	0	0	1.6	-3.2	1.4(5)
S(2)	opposite 6-ring ^c	-2	0	0	1	-2	0.6	-1.2	0.4(3)
O(5)	opposite 4-ring ^a	0	10	0	0	0	4.9	0	5.1(10)
O(4)	opposite 6-ring ^{a,b}	0	0	0	3	0	1.8	0	2.2(4)
Σ(Cd)			6	+12	6	+12	6.0	+12.0	
Σ(Na)			8	+8	2	+2	4.4	+4.4	
Σ(S)			4	-8	1	-2	2.2	-4.4	
Σ(O)			10	0	3	0	5.8	0	
(b) as monatomic and polyatomic cations									
Cd ₆ S ₄ ⁴⁺	Cd(1), Cd(4), S(1)	+4	1	+4	0	0		+1.6	
Cd ₂ Na ₂ S ₄ ⁴⁺	Cd(2), Na(4), S(2)	+4	0	0	1	+4		+2.4	
[Na ₄ O ₈] ⁴⁺	Na(3), O(5)	+4	1	+4	0	0		+1.6	
[NaO] ⁺	Na(2), O(5)	+1	2	+2	0	0		+0.8	
[CdO] ⁺	Cd(3), O(4)	+2	0	0	3	+6		+3.6	
Cd ²⁺		+2	0	0	1	+2		+1.2	
Na ⁺		+1	2	+2	0	0		+0.8	
Σ				+12		+12		+12	

^a In the large cavity. ^b On 3-fold axes. ^c In the sodalite cavity.

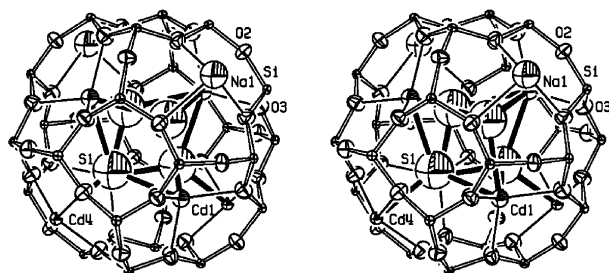


Figure 8. Stereoview of the sodalite cavity of unit cell 1 (UC1) in $[\text{Cd}_{2.4}\text{Na}_{3.2}(\text{Cd}_6\text{S}_4)_{0.4}(\text{Cd}_2\text{Na}_2\text{S})_{0.6}(\text{H}_2\text{O})_{\geq 5.8}][\text{Si}_{12}\text{Al}_{12}\text{O}_{48}]\text{-LTA}$, crystal 1 (hydrated), containing a cationic $\text{Cd}_6\text{S}_4^{4+}$ cluster with a central Cd_4S_4 group. Each Cd^{2+} cation at Cd(1) coordinates octahedrally to three S^{2-} ions at S(1) and three O(3) framework oxygens. Each of two S^{2-} ions coordinates tetrahedrally to three Cd^{2+} cations at Cd(1) and one Cd^{2+} cation at Cd(4). See the caption to Figure 5 for other details.

structure of crystal 2 is only somewhat closer to that of evacuated $\text{Cd}_6\text{-A}$ than to hydrated $\text{Cd}_6\text{-A}^{25}$ (see Table 8), even though both are evacuated.

Per unit cell, six Cd^{2+} and four Na^+ ions are found at seven crystallographic positions. Eight of these ten cations fill the eight 6-rings per unit cell; two Cd^{2+} ions are at Cd(1), one each are at Cd(2) and Cd(3), and two Na^+ ions occupy each of the Na(1) and Na(2) positions (see Figures 10 and 11). The sum of the charges of these eight cations, 12+, balances that of the zeolite framework. The deviations of these ions from the mean (111) plane at O(3) are given in Table 6; it can be seen there that the two Cd^{2+} ions per unit cell at Cd(1) are recessed into the sodalite units from the 6-ring planes while the two at Cd(2) and Cd(3) extend into the large cavities. The two remaining cations, both Cd^{2+} , are in the large cavity, one at Cd(4) on an 8-ring plane and the other at Cd(5) opposite a 4-ring.

The eight 6-ring cations all approach O(3) oxygen atoms of the zeolite framework at reasonable distances. Considering the sum of the conventional ionic radii of Cd^{2+} and O^{2-} , 2.29 Å,³⁰

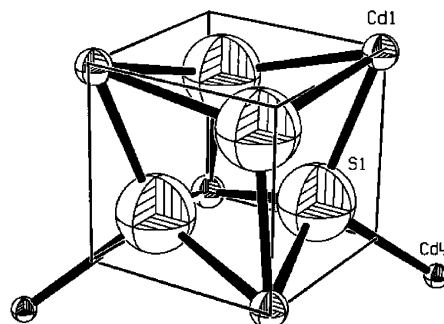


Figure 9. The cationic $\text{Cd}_6\text{S}_4^{4+}$ cluster with a central Cd_4S_4 group with (near) T_d symmetry found in 40% of the sodalite units (UC1) in $[\text{Cd}_{2.4}\text{Na}_{3.2}(\text{Cd}_6\text{S}_4)_{0.4}(\text{Cd}_2\text{Na}_2\text{S})_{0.6}(\text{H}_2\text{O})_{\geq 5.8}][\text{Si}_{12}\text{Al}_{12}\text{O}_{48}]\text{-LTA}$, crystal 1 (hydrated). A cube is drawn with fine lines so that the distortion of the Cd_4S_4 group from cubic can be easily seen. See the caption to Figure 5 for other details.

TABLE 8: (Si,Al)-O-(Si,Al) Angles (deg)^a at Framework Oxygens of Cd^{2+} -Exchanged Zeolite A

Cd^{2+} -exchanged zeolite A	O(1)	O(2)	O(3)
hydrated $\text{Cd}_6\text{-A}^b$	159.0(8)	154.8(10)	143.4(9)
evacuated $\text{Cd}_6\text{-A}^b$	160.9(3)	156.2(6)	137.7(4)
crystal 1 (hydrated)	160.6(5)	158.7(5)	139.0(3)
crystal 2 (dehydrated)	158.2(4)	156.6(4)	138.4(2)

^a The numbers in parentheses are the estimated standard deviations in the units of the least significant digit given for the corresponding parameter. ^b Data from ref 25.

the approach distances of these ions to O(3), 2.262(4), 2.178(4), and 2.281(5) Å, respectively, are reasonable; they are also within the range of those found in previous work (2.16 to 2.39 Å).^{21,25} The Na^+ ions at Na(1) and Na(2) approach the O(3) 6-ring oxygens at 2.389(7) and 2.454(8) Å, respectively, in reasonable agreement with the sum of the ionic radii of Na^+ and O^{2-} , also 2.29 Å,³⁰ and with those found in dehydrated $\text{Na}_{12}\text{-A}$, 2.32 to 2.47 Å.³¹

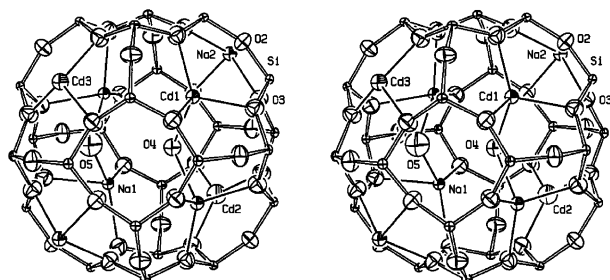


Figure 10. Stereoview of the sodalite cavity in $[\text{Cd}_4\text{Na}_2(\text{Cd}_2\text{O})-(\text{Na}_2\text{O})](\text{Si}_{12}\text{Al}_{12}\text{O}_{48})\text{-LTA}$, crystal 2 (dehydrated). Each sodalite cavity contains a Na_2O molecule and a Cd_2O^{2+} cation as shown. See the caption to Figure 5 for other details.

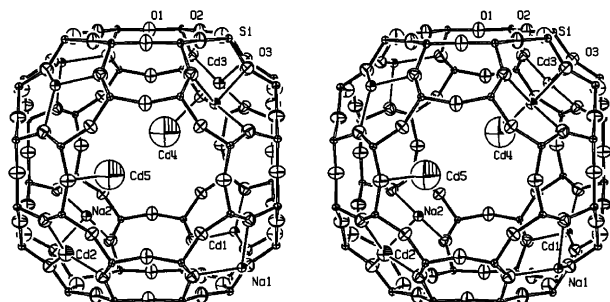


Figure 11. Stereoview of the large cavity in $[\text{Cd}_4\text{Na}_2(\text{Cd}_2\text{O})(\text{Na}_2\text{O})](\text{Si}_{12}\text{Al}_{12}\text{O}_{48})\text{-LTA}$, crystal 2 (dehydrated). See the caption to Figure 5 for other details.

The two remaining non-6-ring Cd^{2+} ions per unit cell do not approach framework oxygens as closely as the 6-ring Cd^{2+} ions approach O(3). The 8-ring Cd(4) ion is 2.59(3) Å from one 8-ring oxygen at O(2) and 2.979(16) Å from two others at O(1) (see Figure 11). Even the shorter of those distances is substantially longer than those found in evacuated $\text{Cd}_6\text{-A}^{25}$ (2.19 to 2.39 Å). However, it is in the range of those in a similarly more complex form of zeolite A, dehydrated $\text{Cd}_{9.5}\text{Cl}_4(\text{OH})_3\text{-A}$ (LTA),²² CdClOH-A , (2.24 to 3.55 Å); actually the 2.59(3)-Å Cd(4) to O(2) distance is the same as the 4-ring Cd(3) ion to O(1) oxygen distance, 2.62(2) Å, in CdClOH-A .²² The 4-ring Cd(5) ion occupies a position similar to that of Cd(3) (0.1516, 0.3501, 0.5) in CdClOH-A .²² Cd(5) is 2.56(4) Å from one O(1) and 3.177(24) Å from two O(2) oxygens; the shorter of these is also the same as the above distances. The closest distances between Cd^{2+} ions and framework oxygens in evacuated $\text{Cd}_6\text{-A}$ (2.19 to 2.39 Å) are shorter than those of Cd(4)–O(2) and Cd(5)–O(1) because all ions in evacuated $\text{Cd}_6\text{-A}$ are 3-fold-axis positions opposite 6-rings. Often 8-ring and 4-ring cations are more distant than 6-ring cations from framework oxygens.²² This is because 8- and 4-rings provide a less adequate (less surrounding) coordination environment to most monatomic cations (see Figure 11), and that is a direct consequence of the poor fit that these cations, except for the very largest, have with these rings. Local framework distortions are likely to be important also.

The sum of the charges of the exchangeable cations per unit cell is 16+ (12+ for six Cd^{2+} + 4+ for four Na^+ ions). Because the anionic charge of the zeolite framework is only 12– per unit cell, guest anions with a total charge of 4– per unit cell are need for charge balance. Nicely, two O^{2-} anions were found at two positions in the sodalite unit, one at O(4) and one at O(5) (see Figure 10). They can be 3.43(9) Å apart, so they can coexist in the same sodalite cavity as shown in Figure 10. An alternative placement, with two O(4) ions in half of the sodalite

cavities and two O(5) ions in the other half, would require an even shorter distance, O(4)–O(4) = 2.90(9) Å, and would provide a less even balance of charge to the zeolite framework.

The oxide ion at O(4) is 2.28(3) Å from two Cd^{2+} ions at Cd(1) (the sum of the corresponding radii = 2.29 Å³⁰). Thus a Cd_2O^{2+} cation is present in each sodalite cavity (Cd(1)–O(4)–Cd(1) = 113.5(22)°, see Figure 10). Each O(5) oxide ion is 2.21(10) Å from two Na^+ ions at Na(1) (the sum of the corresponding radii = 2.29 Å³⁰), thus forming a Na_2O molecule (Na(1)–O(5)–Na(1) = 101(6)°, see Figure 10) in the sodalite cavity.

4.4. Verification of the Atomic Composition of Crystal 2 by SEM-EDX Analysis. The atomic composition of the dehydrated crystal was confirmed using scanning electron microscopy and energy dispersive X-ray analysis (SEM-EDX) (see Table 2). The atomic percentage of each element is consistent with that determined crystallographically, considering the crystallographic esds (see Table 4), the acceptable error range of the EDX analysis, and the sample differences (due to further crystal handling) for the two analyses. The atomic percentage of S, 0.9%, may be regarded as insignificantly different from the crystallographically determined value, 2.4%, because the acceptable error range in SEM-EDX analysis is about 1%. The atomic concentrations of both Cd and Na are also somewhat smaller than those determined crystallographically.

4.5. XPS Analysis of Cd^{2+} in Crystal 2. The main photoelectron peaks corresponding to Cd 3d_{3/2} and 3d_{5/2} are at 412.4 and 405.6 eV, respectively (see Figure 2), when the reference C 1s peak is fixed at 284.3 eV, the value for graphite. The gap between the 3d_{3/2} and 3d_{5/2} binding energies is 6.8 eV, the same as seen in previous work.³⁹ The Cd 3d_{5/2} binding energy, 405.6 eV, is approximately the average of those in Cd metal and Cd^{2+} -exchanged montmorillonite,³⁹ 404.8 and 406.4 eV, respectively.

Each peak (Cd 3d_{3/2} and 3d_{5/2}) of crystal 2 lacks bilateral symmetry (see Figure 2). A multi-fitting operation for the 3d_{5/2} peak at 405.6 eV using a Gaussian model indicates the presence of two sub-peaks at 405.6 and 406.3 eV. The ratio of their areas is 2.1, in agreement with 2.0, the ratio of the occupancies of the Cd^{2+} ions bonded to framework oxygens only, to those bound to both framework and guest oxides (O(4)), as determined crystallographically (see section 4.2.). Furthermore, the higher binding energy at 406.3 eV is reasonable; as more oxygens coordinate, the XPS peaks of metal atoms shift to higher energy. XPS has confirmed that the dehydrated crystal contains two nonequivalent kinds of Cd^{2+} cations in a 2:1 ratio.

A smaller Cd 3d_{5/2} binding energy, 404.6 eV (when the reference C 1s peak is fixed at 284.3 eV), was found for CdS thin films on borosilicate glass.⁴⁰ This value is generally smaller for sulfides as compared to oxides, and 404.6 eV is reasonable. That each peak (Cd 3d_{3/2} and 3d_{5/2}) is a single line indicates that all Cd^{2+} ions there are equivalent as expected.

4.6. Determination of the Thermal Stability of the CdS-Containing Nanoclusters.

4.6.1. Powder XRD and TGA Results. Both powder XRD at various temperatures (see Figure 3) and TGA (see Figure 4) indicate that the CdS-containing clusters in hydrated CdNaS-A powder are stable below 673 K in air and below 1073 K in nitrogen. In agreement, the CdNaS-A powder remained yellow after these treatments. However, these clusters are oxidized at some temperature above 673 K in air (see Figures 3 and 4). In agreement, the color of the sample changed from yellow to white when it was heated from 673 to 1073 K in air during TGA. The same color change was seen when bulk CdS powder was

heated in air from 673 to 1073 K. (When crystal 1 was dehydrated at 623 K in vacuum to become crystal 2 (see section 2.1.), its color also became much lighter; it changed from dark yellow to pale yellow.)

The thermal stability of CdNaS-A was examined by TGA from 318 to 1073 K in air and in nitrogen, with fully Cd^{2+} -exchanged zeolite A powder (Cd-A) as a reference (see Figure 4). As expected due to water desorption, the weights of all samples decreased by about 11–15% as the temperature rose to 473 K. Above 473 K in air, the weight of the CdNaS-A powder slowly decreased until 673 K and then increased from ca. 700 to 973 K as its color changed from yellow to white. In contrast, the weights of the CdNaS-A powder in nitrogen and Cd-A powder in air slowly decreased in the range 473–973 K and their colors did not change. This behavior indicates that no chemical reaction (such as oxidation) occurred with CdNaS-A in nitrogen nor Cd-A in air. We may conclude that CdNaS-A reacted with air above ca. 700 K. It appears that CdS -containing groups have reacted with oxygen. The mass increase is attributed to the retention of oxidized sulfur, perhaps as sulfate⁴¹ (see section 4.7.1). This is consistent with a color change from CdS (yellow) to CdSO_4 (colorless). (Note that crystal 1, when heated to 623 K in the absence of air to become crystal 2, remained pale yellow. A corresponding powder might well have appeared white. All sulfide had been lost; only oxides remained; bulk CdO is brown.

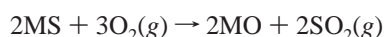
Using the approximate unit-cell formula $\text{Cd}_6\text{Na}_{4.4}\text{S}_{2.2}\text{Si}_{12}\text{Al}_{12}\text{O}_{48}\cdot 30\text{H}_2\text{O}$, MW = 2815, for CdNaS-A , and a mass increase of $88.2\% - 85.4\% = 2.8\%$ upon heating CdNaS-A from 700 to 1073 K in air (see Figure 4), it can be calculated that about five oxygen atoms were added per unit cell from the atmosphere. This is less than the 8.8 oxygens that would have been needed to transform the 2.2 sulfide ions to sulfate. Perhaps the difference is due to the partial decomposition of sulfite or sulfate; some sulfur may have been lost as SO_2 or SO_3 .

A comparison of the powder diffraction pattern of CdNaS-A (hydrated) with that of Cd-A (hydrated) (see Figure 3) shows that the structure of Cd-A had changed significantly after treatment with Na_2S , indicating that a significant number of atoms had been introduced into the zeolite. It can also be seen in Figure 3 that the zeolite framework of CdNaS-A had largely decomposed after heating to 1073 K in air.

4.6.2. Single-Crystal XRD Results. During the vacuum-dehydration process, per unit cell, the number of Na^+ ions decreased from 4.4 to 4.0, the number of locatable nonframework oxygens from 5.8 to 2.0, and the number of sulfide ions from 2.2 to 0. During this process the number of Cd^{2+} ions and those of all framework elements remained constant. These numbers, and the structure of crystal 2, show that vacuum-dehydration at 623 K had decomposed both sulfide-containing clusters, $\text{Cd}_6\text{S}_4^{4+}$ and $\text{Cd}_2\text{Na}_2\text{S}^{4+}$, leaving one Na_2O and one Cd_2O^{2+} group per unit cell

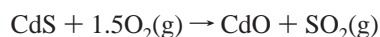
4.7. Oxidation of Cadmium Sulfide upon Heating.

4.7.1. With Air or Oxygen. The powder TGA result, that sulfates and perhaps oxides have formed from sulfides upon heating in air or oxygen, has precedent. Sulfide ores such as MnS , FeS , ZnS , PbS , NiS , Cu_2S , and CdS are roasted in air to give oxides.^{42,43} Greenockite, CdS , is always associated with zinc-lead sulfide ores; this mixture when roasted in air gives ZnO , PbO , and CdO ⁴⁴



CdS films annealed in air at 573 K for 30 min were oxidized; X-ray photoelectron spectroscopy showed that their surfaces

consisted predominantly of CdO - and CdSO_4 -like species.⁴¹ A thin layer of CdO was formed on a chemically deposited CdS thin film through reaction with atmospheric oxygen by heating in air for 5 min at 643 to 773 K.⁴⁵ A porous $\text{CdS}:\text{CdO}$ composite structure was formed on a CdS matrix after sintering in air at high temperature.⁴⁶ The reactions



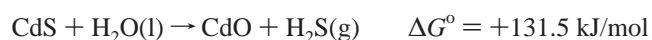
$$\Delta G^\circ = -372.3 \text{ kJ/mol}$$

or



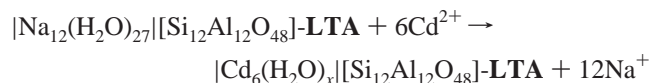
are strongly exoergic.⁴⁷

4.7.2. With Water. The single-crystal crystallographic result, that oxides have formed from sulfides upon heating under vacuum in the presence of intrazeolitic water, is somewhat endoergic at 298.15 K⁴⁷

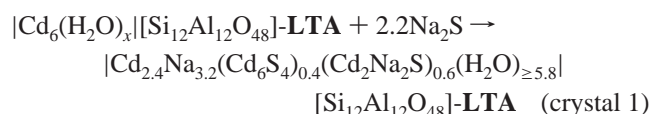


The greater volatility (weaker coordination to cations) of H_2S as compared to H_2O appears to have driven this reaction to completion by mass action as the temperature was increased under dynamic vacuum during the “dehydration” of crystal 1. As in section 4.7.1., this calculation of ΔG° overlooks the thermodynamic differences between small CdS - and CdO -containing clusters and the pure solid CdS and CdO phases.

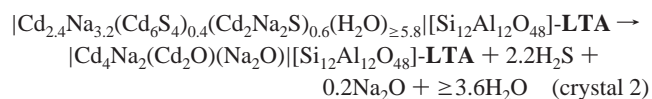
4.8. Net Reactions. The reaction per unit cell upon ion exchange of $\text{Na}_{12}\text{-A}$ (LTA) with aqueous 0.05 M Cd^{2+} , followed by washing with water, both at 294 K, appears to be



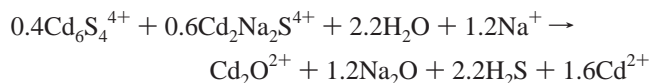
The reaction per unit cell upon further treatment with aqueous 0.05 M Na_2S at 294 K appears to be



Finally, the reaction per unit cell upon vacuum dehydration at 623 K appears to be



For this last step, the net reaction per unit cell is



Of the 1.2 Na_2O molecules formed per unit cell, 0.2 appear to have exited the zeolite structure. This is reasonable because Na_2O is mobile/volatile at 623 K and because a suitable position for it within the zeolite structure is not available.

It is interesting to see that both Na_2O and Cd_2O^{2+} remained in the zeolite at 623 K to the maximum capacity at their preferred sites. Only the excess Na_2O and no CdO moved to the surface of the zeolite single crystal.

5. Summary

In hydrated $[\text{Cd}_{2.4}\text{Na}_{3.2}(\text{Cd}_6\text{S}_4)_{0.4}(\text{Cd}_2\text{Na}_2\text{S})_{0.6}(\text{H}_2\text{O})_{\geq 5.8}][\text{Si}_{12}\text{Al}_{12}\text{O}_{48}]\text{-LTA}$, $\text{Cd}_6\text{S}_4^{4+}$ nanoclusters with a Cd_4S_4 core (interpenetrating tetrahedra) have been found in about 40% of the sodalite cavities. The remaining 60% each contain a planar $\text{Cd}_2\text{-Na}_2\text{S}^{4+}$ cluster. Vacuum dehydration at 623 K causes both clusters to lose all sulfur and to be converted to one Cd_2O^{2+} cation and one Na_2O molecule in each sodalite cavity of $[\text{Cd}_4\text{-Na}_2(\text{Cd}_2\text{O})(\text{Na}_2\text{O})][\text{Si}_{12}\text{Al}_{12}\text{O}_{48}]\text{-LTA}$. Both CdS-containing nanoclusters in $[\text{Cd}_{2.4}\text{Na}_{3.2}(\text{Cd}_6\text{S}_4)_{0.4}(\text{Cd}_2\text{Na}_2\text{S})_{0.6}(\text{H}_2\text{O})_{\geq 5.8}][\text{Si}_{12}\text{Al}_{12}\text{O}_{48}]\text{-LTA}$ appear to be stable in air up to ca. 700 K. This great stability is given by the zeolite structure as discussed in the Introduction (paragraph 1 of section 1).

Acknowledgment. This work was supported by a Korea Research Foundation Grant funded by the Korean Government (MOEHRD) (KRF-2005-041-D00223). We are grateful to the Pohang Accelerator Laboratory at POSTECH for allowing us to use their diffractometer and computing facilities.

Supporting Information Available: Tables of observed and calculated structure factors squared with esds for crystals 1 and 2. This material is available free of charge via the Internet at <http://pubs.acs.org>.

References and Notes

- (1) Bhatia, S. *Zeolite Catalysis: Principles and Applications*; CRC Press: Boca Raton, FL, 1988; pp 1–2.
- (2) Smith, J. V. *Am. Chem. Soc. Monogr.* **1976**, 171, 3.
- (3) Srdanov, V. I.; Blake, N. P.; Markgraber, D.; Metiu, H.; Stucky, G. D. *Advanced Zeolite Science and Applications: Stud. Surf. Sci. Catal.* **1994**, 85, 115.
- (4) Terasaki, L.; Yamazaki, K.; Thomas, J. M.; Ohsuna, T.; Watanabe, D.; Sanders, J. V.; Barry, J. C. *Nature (London)* **1987**, 330, 58.
- (5) Stucky, G. D.; MacDougall, J. E. *Science* **1990**, 247, 669.
- (6) Alekseev, Yu. A.; Bogomolov, V. N.; Zhukova, T. B.; Petranovskii, V. P.; Romanov, S. G.; Kholodkevich, S. V. *Izv. Akad. Nauk SSSR, Ser. Fiz.* **1986**, 50, 418.
- (7) Wang, Y.; Herron, N. J. *Phys. Chem.* **1987**, 91, 257.
- (8) Wang, Y.; Herron, N. J. *Phys. Chem.* **1988**, 92, 4988.
- (9) Herron, N.; Wang, Y.; Eddy, M. M.; Stucky, G. D.; Cox, D. E.; Moller, K.; Bein, T. *J. Am. Chem. Soc.* **1989**, 111, 530.
- (10) Fukuoka, A.; Sakamoto, Y.; Guan, S.; Inagaki, S.; Sugimoto, N.; Fukushima, Y.; Hirahara, K.; Iijima, S.; Ichikawa, M. *J. Am. Chem. Soc.* **2001**, 123, 3373.
- (11) Chen, W.; Wang, Z.; Lin, Z.; Lin, L.; Fang, K.; Xu, Y.; Su, M.; Lin, J. *J. Appl. Phys.* **1998**, 83, 3811.
- (12) Stramel, R. D.; Nakamura, T.; Thomas, J. K. *Chem. Phys. Lett.* **1986**, 130, 423.
- (13) Jentys, A.; Grimes, R. W.; Gale, J. D.; Catlow, C. R. A. *J. Phys. Chem.* **1993**, 97, 13535.
- (14) Ochoa-Landin, R.; Flores-Acosta, M.; Ramirez-Bon, R.; Arizpe-Chavez, H.; Sotelo-Lerma, M.; Castillon-Barraza, F. F. *J. Phys. Chem. Solids* **2003**, 64, 2245.
- (15) Chen, W.; Xu, Y.; Lin, Z.; Wang, Z.; Lin, L. *Solid State Comm.* **1997**, 105, 129.
- (16) Yahiro, H.; Kyakuno, T.; Okada, G. *Top. Catal.* **2002**, 19, 193.
- (17) Breck, D. W. *Zeolite Molecular Sieves*; Wiley: New York, 1974.
- (18) *Preparation of Catalyst III*; Poncelet, G., Grange, P., Jacobs, P. A., Eds.; Elsevier Science: Amsterdam, 1983.
- (19) Charnell, J. F. *J. Cryst. Growth* **1971**, 8, 291.
- (20) Gramlich, V.; Meier, W. M. *Z. Kristallogr.* **1971**, 133, 134.
- (21) Song, M. K.; Kim, Y.; Seff, K. *J. Phys. Chem. B* **2003**, 107, 3117.
- (22) McCusker, L. B.; Seff, K. *J. Am. Chem. Soc.* **1978**, 100, 5052.
- (23) Mellum, M. D.; Seff, K. *J. Phys. Chem.* **1984**, 88, 3560.
- (24) Sheldrick, G. M. *SHELXL97, Program for the Refinement of Crystal Structures*; University of Göttingen: Göttingen, Germany, 1997.
- (25) McCusker, L. B.; Seff, K. *J. Phys. Chem.* **1981**, 85, 166.
- (26) Doyle, P. A.; Turner, P. S. *Acta Crystallogr. Sect. A* **1968**, 24, 390.
- (27) *International Tables for X-ray Crystallography*; Kynoch Press: Birmingham, England, 1974; Vol. IV, pp 71–98.
- (28) Cromer, D. T. *Acta Crystallogr.* **1965**, 18, 17.
- (29) *International Tables for X-ray Crystallography*; Kynoch Press: Birmingham, England, 1974; Vol. IV, pp 148–150.
- (30) *Handbook of Chemistry and Physics*, 64th ed.; The Chemical Rubber Co.: Cleveland, OH, 1983; p F-170.
- (31) Yanagida, R. Y.; Amaro, A. A.; Seff, K. *J. Phys. Chem.* **1973**, 77, 805.
- (32) Armstrong, A. R.; Anderson, P. A.; Woodall, L. J.; Edwards, P. P. *J. Am. Chem. Soc.* **1995**, 117, 9087.
- (33) Heo, N. H.; Chun, C. W.; Park, J. S.; Lim, W. T.; Park, M.; Li, S.-L.; Zhou, L.-P.; Seff, K. *J. Phys. Chem. B* **2002**, 106, 4578.
- (34) Heo, N. H.; Park, J. S.; Kim, Y. J.; Lim, W. T.; Jung, S. W.; Seff, K. *J. Phys. Chem. B* **2003**, 107, 1120.
- (35) Seff, K. *Microporous Mesoporous Mater.* **2005**, 85, 351.
- (36) Yeom, Y. H.; Kim, Y.; Seff, K. *Microporous Mesoporous Mater.* **1999**, 28, 103.
- (37) Lee, Y. M.; Jeong, G. H.; Kim, Y.; Seff, K. *Microporous Mesoporous Mater.* **2006**, 88, 105.
- (38) Sun, T.; Seff, K. *J. Phys. Chem.* **1993**, 97, 7719.
- (39) *Handbook of X-ray Photoelectron Spectroscopy: a Reference Book of Standard Data for Use in X-ray Photoelectron Spectroscopy*; Perkin-Elmer Co.: Eden Prairie, MN, 1979; pp 114–115.
- (40) Stoev, M. D.; Tousek, J.; Tousek, J. *Thin Solid Films* **1997**, 299, 67.
- (41) Kolhe, S.; Kuljarni, S. K.; Nigavekar, A. S.; Sharma, S. K. *Solar Energy Mater.* **1984**, 10, 47.
- (42) Moore, J. J. *Chemical Metallurgy*, 2nd ed.; Butterworth-Heinemann Ltd.: Jordan Hill, Oxford, 1990; pp 250–254.
- (43) Newton, J. *Extractive Metallurgy*; John Wiley and Sons, Inc.: New York, 1959; pp 285–287.
- (44) Jezowska-Trzebiatowska, B.; Kopacz, S.; Mikulski, T. *The Rare Elements: Occurrence and Technology*; Elsevier Science Publishing Co., Inc.: New York, 1990; pp 270–271.
- (45) Nair, P. K.; Daza, O. G.; Readigos, A. A.; Campos, J.; Nair, M. T. *S. Semicond. Sci. Technol.* **2001**, 16, 651.
- (46) Sebastian, P. J.; Calixto, M. E. *Thin Solid Films* **2000**, 360, 128.
- (47) *Handbook of Chemistry and Physics*, 75th ed.; The Chemical Rubber Co.: Cleveland, OH, 1994; pp 5-9–5-22.